Poly(butylene succinate) ionomers and their use as compatibilizers in nanocomposites

Mayka Bautista, Antxon Martínez de Ilarduya, Abdelilah Alla, and Sebastián Muñoz-Guerra*

Universitat Politècnica de Catalunya, Departament d´Enginyeria Química,
ETSEIB, Diagonal 647, Barcelona 08028, Spain

Abstract

A series of low molecular weight poly(butylene succinate-*co*-glutarate-*co*-2-trimethylammonium chloride glutarate) terpolyester ionomers containing 35%-mol of total glutarate units but varying in the content of charged units were synthesized by polycondensation at mild temperatures using a scandium catalyst. The terpolyester ionomers started to decompose at temperatures above 175 ºC, all they were semicrystalline and have T_g similar to PBS. These terpolyesters were used to compatibilize the nanocomposites made of poly(butylene succinate)-cloisite (PBS·CL) prepared by melt extrusion. XRD revealed that an intercalated structure was present in these nanocomposites. The thermal properties of the three-component mixtures did not differ substantially from those of PBS·CL but the mechanical properties were significantly improved by addition of the ionomer, in particular tenacity. The beneficial effect afforded by the terpolyester ionomer was attributed to its ability for strengthening the binding between PBS and the nanoclay.

INTRODUCTION

Poly(butylene succinate) (PBS) is a well-known aliphatic polyester that is synthesized from succinic acid (SA) and 1,4-butanediol (BD) in a variety of grades to give response to a wide assortment of applications. This polyester exhibits a balanced performance in thermal and mechanical properties, as well as a thermoplastic processability comparable to other common plastics [1-3]. The production of the PBS monomers from renewable resources is rapidly advancing so that this polyester is breaking through other polyesters of widely recognized sustainability such as poly(lactic acid) [4] and poly(hydroxyalkanoate)s [5]. Today bio-based PBS is a good candidate to be ecofriendly used in high tonnage applications such as packaging, non-wovens, and mulch films. On the other hand, PBS is comparable to other biodegradable polyesters such as poly(ε-caprolactone) and poly(glycolic acid) regarding its potential as a biomaterial for temporal applications. Nevertheless the T_g and mechanical behavior of PBS are far from what it would be desirable, in particular when aromatic polyesters are concerned, a drawback that is hampering its penetration in some fields traditionally occupied by fossil thermoplastics.

Layered silicate nanocomposites have been proposed as a good option to improve the physical properties of aliphatic polyesters and they are emerging as the next generation of biodegradable materials [6-8]. Someya *et al*. [8] prepared nanocomposites made of PBS and organo-modified montmorillonites by melt intercalation and subsequent injection molding. These nanocomposites displayed a high degree of intercalation and showed tensile and flexural moduli higher than PBS but lower tensile strength. Ray *et al.* [9] reported on the same type of nanocomposites prepared by simple melt extrusion. Also a good intercalation of the silicate layers into the polymeric matrix was attained by this method and the nanocomposites also exhibited remarkably improved mechanical properties in both solid and melt states compared with neat PBS. Nevertheless, all PBS nanocomposites containing nanoclays are found to be significantly less tough than the polyester because flowing at high deformations becomes largely restricted, an effect that is a commonly observed in polymer

nanocomposites. Strikingly this effect is not observed in nanocomposites of poly(butylene succinate-*co*-adipate) made of Cloisite 30B obtained by melt-extrusion, which exhibited substantial increase in both stiffness and elongation at break compared to the copolyester [10]. It seems therefore that a high degree of intercalation is not enough to provide a general improvement of the mechanical behavior of PBS nanocomposites but that a deeper interaction polymer-silicate has to be also attained.

The ionomer concept has been also employed to improve some aspects of the mechanical behavior of polymers and in particular to get better interactions with charged fillers in nanocomposites [11,12]. Han *et al*. [13,14] reported a series of poly(butylene succinate) ionomers containing 5-sodium sulfoisophthalate units prepared by bulk polycondensation. The presence of small amounts of sulfonate groups in PBS provided higher melt viscosity and improved significantly certain thermal and mechanical properties. However the ionomer structure unavoidably entails a decrease in crystallinity, an effect that is especially detrimental for aliphatic polyesters displaying low or moderate glass transition and melting temperatures, as it is the case of PBS.

In this work, an ionomer is designed and synthesized to be used as compatibilizer in PBS/cloisite nanocomposites prepared by melt extrusion. The ionomer is a PBS terpolyester ($PBS_xG_yG^I_z$) containing minor amounts of glutarate units both unmodified and modified with a trimethylammonium group attached to the α-backbone carbon. It is expected that this ionomer is able to interact strongly with the nanoclay creating an in situ organomodified montmorillonite with good accessibility to PBS. Several nanocomposite compositions varying in the ionomer content and the PBS/compatibizer or the PBS/nanoclay ratios have been prepared and their thermal and mechanical properties comparatively evaluated in order to appraise the effect of the compatibilizer on the PBS/cloisite nanocomposites.

EXPERIMENTAL

Materials

Succinic acid (SA) (99%) was purchased from Panreac. 1,4-Butanediol (99%), scandium (III) trifluoromethanesulfonimide ($Sc(NTf_2)_3$), potassium *tert*-butoxide, iodomethane, L-glutamic acid dimethyl ester hydrochloride and glutaric acid (GA) were purchased from Sigma-Aldrich. Solvents used for purification and characterization as diethyl ether, chloroform, hexane, or acetonitrile, and dichloroacetic and trifluoroacetic acids were purchased from Panreac. All they were of either technical or high-purity grade and used as received without further purification. Unmodified sodium montmorillonite (cloisite) was supplied by Southern Clay Products.

Measurements

Intrinsic viscosities of the copolyester dissolved in dichloroacetic acid were measured with and Ubbelohde viscometer thermostated at 25 ºC ± 0.1 ºC. Size exclusion chromatography (SEC) was performed on a Waters system equipped with a refractive index detector (RID-10A) using 1,1,1,3,3,3-hexafluoro-2-propanol as the mobile phase. Molecular weights and their distribution were calculated against poly(methyl methacrylate) standards using the Millenium 820 software. To prevent ionic aggregation, polymer samples were previously dissolved in a mixture of chloroform/trifluoroacetic acid (1/1) and precipitated with methanol.

NMR spectra were recorded on a Bruker AMX-300 spectrometer operating at 300.1 MHz for ^{1}H and 75.5 MHz for ^{13}C. About 10 mg for ^{1}H or 50 mg for ^{13}C of polymer samples were dissolved in 1 mL of mixture of deuterated chloroform ($CDCl_3$) and trifluoroacetic acid (TFA) (7/3 v/v). 64 and 5000–10,000 scans were acquired with 32- and 64-K data points and 1 and 2 sec of relaxation delays for ^{1}H and ^{13}C, respectively. The thermal behavior of the polyesters was examined by differential scanning calorimetry (DSC) with a PerkinElmer DSC Pyris 1 instrument calibrated with indium and zinc for the temperature and enthalpy. DSC data were obtained from 4 to 6 mg samples at heating and cooling rates of 10ºC min^{-1} under

nitrogen circulation (20 mL min^{-1}). T_g of polyesters and nanocomposites were measured from amorphous samples at heating rate of 20ºC min^{-1}. TGA measurements were performed from 10 to 15 mg of sample under a nitrogen flow of 20 mL min^{-1} at a heating rate of 10 ºC min^{-1} and within a temperature range of 30–600 ºC for polyesters and 30-800ºC for nanocomposites, using a Perkin-Elmer TGA6 thermobalance. Tensile testing was performed on bone shape specimens (2.7x10 mm^2) which were cut from isotropic films obtained by hot pressing with a thickness of about 200 μm. Tensile tests were conducted at room temperature on a Zwick BZ2.5/TN1S universal tensile testing apparatus operating at a constant crosshead speed of 10 mm min^{-1} with a 0.5 N preload and a grip-to-grip separation of 20 mm. Five measurements were made for each polymer and results are reported as average values. X-ray diffraction patterns were recorded on the PANalytical X'Pert PRO MPD θ/θ diffractometer using the Cu Kα radiation of wavelength 0.1542 nm from powdered samples coming from synthesis. For the preparation of the nanocomposites a twin screw mini-extruder (Haake, Minilab) operating in counter-rotation with a speed of 75 rpm was used.

Synthesis

2-(*N,N,N*-trimethylammonium)-glutaric acid chloride (TMAGA·Cl). 2-(*N,N,N*-trimethylammonium)-glutaric acid chloride was synthesized according to the general procedure described in the literature for quaternization of amines [15]. Efficient quaternization of L-glutamic acid dimethyl ester was attained by using iodomethane in methanol. The reaction was carried out by stirring a mixture of 20 g of iodomethane, 4 g of $NaHCO_3$ and 1 g of glutamic acid dimethyl ester in 100 mL of methanol at room temperature for 24 h. The residue left after evaporation to dryness of the reaction mixture was extracted with $CHCl_3$ and the extract was evaporated to give a solid that was crystallized from chloroform-hexane solution (80/20). The obtained 2-(*N,N.N*-trimethylammonium) dimethyl glutarate iodide (TMAMG·I) was subjected to basic hydrolysis. The hydrolysis process was

monitored by NMR by following the decreasing of the methoxy proton signal so that the reaction was considered to be finished when no trace of this group was observed in the spectra, which took about 5 h. The aqueous basic solution was acidified with concentrated HCl and then evaporated to dryness at 40 ºC. The solid residue was extracted with acetone and TMAGA·Cl was recovered from the extract upon evaporation.

$PBS_xG_yG^I_z$ terpolyesters. Poly(butylene succinate-*co*-glutarate-*co*-2-trimethylammonium glutarate chloride) ($PBS_xG_yG^I_z$) terpolyesters were prepared according to the synthetic route depicted in Scheme I. A mixture of the three diacids (SA, GA and TMAGA·Cl), 1,4-butanediol and catalyst ($Sc(NTf_2)_3$) with the adjusted proportions was dissolved in acetonitrile (3 mL) in a three-necked cylindrical round-bottom flask equipped with a mechanical stirrer. The acetonitrile was used to obtain a good mixture of the monomers. A 1:1 molar ratio of BD to the total of diacids with 0.3%-mole of $Sc(NTf_2)_3$ respect to monomers) was used. The esterification reaction was left to proceed at 80 ºC under a nitrogen atmosphere for a period of 35-40 h, along which water and acetonitrile were continuously distilled out. Then the polycondensation reaction was initiated by raising the temperature up to 90 ºC and reducing the pressure down to 0.03 mbar. After 100 h a viscous mass was formed which was cooled down to room temperature and the atmospheric pressure in the flask restored with a nitrogen flow to prevent degradation. The final solid mass was used for characterization and properties evaluation without any further treatment.

Preparation of PBS·CL·w%($PBS_{65}G_{20}G^I_{15}$) nanocomposites. Mixtures of PBS, and $PBS_{65}G_{20}G^I_{15}$ terpolyester ionomer at concentrations of 5, 10 and 20% (w/w), all they containing 3% (w/w) of cloisite were extruded in a miniextruder machine at a temperature 10 °C above the melting temperature of PBS for a residence time of 20 min and with the screw rotating rate fixed at 75 rpm.

RESULTS AND DISCUSSION

Synthesis and chemical characterization of $PBS_xG_yG^I_z$ terpolyester ionomer

The synthesis pathway leading to the **$PBS_xG_yG^I_z$** terpolyester ionomers is shown in Scheme I. Acetonitrile was the solvent of choice since it afforded a homogeneous mixture of the initial reaction mixture. The procedure consists of two successive steps, the first one is an esterification reaction leading to low molecular weight oligomers, and the second one is the polycondensation of the oligomers formed in the previous step to render the final terpolyesters. The first step was carried out at 80 ºC with removal of the released water and acetonitrile and the second one was carried out at higher temperatures under high vacuum to speed up the esterification reaction and to favor the removal of water in order to unbalance the equilibrium towards the formation of high molecular weight polymers. Scandium (III) trifluoromethane sulfonimide was chosen as catalyst according to recent literature [16], since it has been reported to be active at relatively low temperatures. In fact, the use of low reaction temperatures is an essential requirement for these polycondensations to proceed successfully since temperatures above 100 ºC promote the thermal decomposition of TMAGA·Cl. All the terpolyesters were obtained in high yields (~90%) but with rather low molecular weights (Table 1). The intrinsic viscosity of $PBS_xG_yG^I_z$ ranged between 0.41 and 0.44 dL g^{-1}.

Scheme I.

The chemical structure and composition of $PBS_xG_yG^I_z$ terpolyesters was ascertained by NMR spectroscopy assisted by COSY 2D NMR spectrum for signal assignment. The ^1H and ^{13}C NMR spectra of $PBS_{65}G_{25}G^I_{10}$ are shown in Figure 1 as a representative of the series. The chemical composition was determined by integration of signals appearing at ~2 ppm for the central CH_2 of the glutarate unit, at ~3.3 ppm for the CH_3 of the trimethylammonium glutarate unit and at ~2.7 ppm arising from the CH_2 of the succinate unit.

Table 1

Results are listed in Table 1 which shows that the content of the terpolyesters in trimethylammonium glutarate units was in general slightly lower than in the feed. The small differences must be attributed to the elimination of the trimethylammonium taking place by effect of heating during the polycondensation reaction.

Figure 1

XRD analysis

The crystalline structure of the copolyesters and the dispersion degree of the nanocomposites was examined by X-ray diffraction. Representative XRD profiles are depicted in Figure 2 together with that produced by cloisite for comparison. The diffraction pattern of cloisite is well known to consist of a main reflection close to 1.0-1.1 nm corresponding to the interlayer spacing together with a series of wide-angle reflections arising from the aluminum silicate crystalline lattice [17]. On the other hand semicrystalline PBS is characterized by a diffraction pattern containing three strong reflections at 0.45, 0.40, and 0.39 nm produced by the monoclinic crystal structure adopted by this polyester [18]. The XRD profiles obtained from the nanocomposites both from PBS alone and from PBS blended with 20% of either the PBSG copolyester or the PBSGG^{I} ionomer are very similar, and all of them display the reflection characteristic of PBS indicating that the crystalline structure of the homopolyester is fully retained not only in the copolyesters but also in the mixtures with the clay. The presence of the intercalated structure in the nanocomposites is evidenced by the displacement towards smaller angle observed for the ~1.0 nm montmorillonite peak which appears in the mixtures around 1.25 nm. Since the intensity and position of this peak is practically the same for the three samples it can be concluded that a similar intercalation degree is attained in the three cases.

Figure 2

Thermal properties

The effect exerted by the incorporation of glutarate units on the thermal properties of PBS was assessed by TGA and DSC. TGA essays addressed to evaluate the thermal stability were conducted under a nitrogen atmosphere in a temperature range of 30-600 ºC. The TGA heating traces registered for $PBS_xG_yG^I_z$ terpolyesters are shown in Figure 3a together with the trace obtained for PBS that is included for comparison. Derivative curves showing the maximum decomposition rates for PBS and the $PBS_{65}G_{20}G^I_{15}$ are compared in Figure 3b. The characteristic decomposition data afforded by TGA are collected in Table 2 which reveal that the thermal stability of the terpolyesters is significantly lower than that of PBS with the ${}^oT_d$ going down near to 90 ºC for the polymer containing 35% of glutarate units. Although a decreasing in molecular weight will be in part responsible for the loss of thermal stability observed for the terpolyesters, it is unquestionable that decomposition temperatures, both the onset and the maximum rate, decrease steadily with the content in G ad G^I units. Furthermore, the insertion of glutarate units makes that decomposition proceeds through two stages with maximum decomposition rates at around 355 and 400 ºC, respectively, whereas PBS decomposes in one single step at 408 ºC. It is concluded therefore that the insertion of G and G^I units in PBS not only decreases its thermal stability but also makes more complex the decomposition mechanism.

Figure 3.

For the determination of the thermal stability of the nanocomposites, TGA measurements were carried out under an oxidative atmosphere over a temperature range of 30-800 ºC. The TGA traces recorded from nanocomposites made from PBS containing Cloisite with and without compatibilizer are shown in Figure 4, and the decomposition data afforded by this analysis are compared in Table 2. The results reveal that the addition of 3% of Cloisite slightly modifies the thermal stability of PBS but has a significant beneficial effect on the thermal behavior of the ionomer terpolymers. In fact the onset decomposition

temperature of PBS·CL containing 3% of nanoclay is 7 ºC higher than that of PBS whereas the maximum decomposition rate temperature is essentially the same. Such slightly beneficial effect of the clay on the thermal stability of PBS has been previously reported [19]. When the $PBS_{65}G_{20}G^{I}_{15}$ terpolyester is added to the PBS·CL mixture, the resulting nanocomposites show a single decomposition process practically undistinguishable from that observed for PBS·CL (Figure 4b). Furthermore the $^{max}T_d$ observed for these three component nanocomposites hardly change with the content in ionomer. What is particularly relevant is the behavior observed for the onset temperature which was found to be about 40 ºC higher than those of the isolate terpolyester ionomers. The fact that the TGA traces of the three-components nanocomposites do not show any sign characteristic of their ionomeric counterpart, leads to concluded that the interaction of the PBS with the terpolyester in the presence of Cloisite must be highly efficient.

Figure 4

The DSC data obtained for the $PBS_xG_yG^{I}_z$ series studied in this work are collected in Table 2. T_g values of $PBS_xG_yG^{I}_z$ terpolyesters increased from -45 to -38 with the content in trimethylammonium glutarate units and T_g values of PBS·CL·w%$PBS_{65}G_{20}G^{I}_{15}$ showed an almost imperceptible decrease with the increase of ionomer content. The DSC traces obtained from the terpolyester series upon heating the molten samples are comparatively depicted in Figure 5. All $PBS_xG_yG^{I}_z$ are semicrystalline with melting temperatures and enthalpies increasing slightly with the content in trimethylammonium groups but always significantly lower than the values measured for PBS. On the other hand, the crystallizability of the terpolyesters, estimated on the basis of the crystallization temperature and enthalpy, was found to be also considerably lower than that of PBS. Furthermore, it is worthy to note the depression appearing on the second heating trace of $PBS_xG_{25}G^{I}_{10}$ at around 15 ºC due the occurrence of cold crystallization. As it is seen in Table 2, the crystallization enthalpy of this polyester is considerably low and therefore a large amount of uncrystallized material remained after cooling. No sign of cold crystallization was detected for any other polyester.

Interestingly the DSC behavior of the three-components nanocomposites regarding both melting and crystallization, did not differ substantially from that of PBS neither in the presence nor the absence of compatibilizer. What can be inferred from these results is that the nucleating effect exerted by the nanoclay is determinant of the crystallization process of PBS either in the presence or absence of ionomer.

Figure 5.

Stress-strain mechanical behavior

The mechanical parameters of the terpolyesters and nanocomposites are listed in Table 2 and the stress-strain curves of the latter are depicted in Figure 6 together with that of PBS. It is apparent that the mechanical behavior of the ionomer terpolyesters is largely poorer than that of PBS, which is undoubtedly consequence of their low molecular weight.

Figure 6

Nevertheless, the Young's modulus (E), elongation at break (ε) and maximum tensile stress (σ_{max}) of terpolyesters tend to increase steadily with the content in G^I units bringing into evidence the positive effect of the presence of charges on mechanical properties, an effect that has been repeatedly reported for other related systems [13]. On the other hand, the nanocomposite prepared by extruding PBS with 3% of cloisite shows enhanced Young's modulus and maximum tensile stress but a largely reduced deformation at break. This is a result commonly found for those nanocomposites that are unable to attain the exfoliated state [20, 21]. The addition of the ionomer $PBS_{65}G_{20}G^I_{15}$ as compatibilizer was shown to clearly improve the mechanical parameters of the PBS nanocomposite. Not only the modulus and yield increased but in particular the ductility was greatly enhanced. In fact, the nanocomposite containing 20% of ionomer could be stretched about ten times more than the nanocomposite without compatibilizer. Comparison with the nanocomposites containing the

copolyester $PBS_{65}G_{35}$, *i.e.* containing the same amount of glutarate units but without ammonium groups, was very enlightening. The presence of such copolyester in PBS·CL produced a moderate increment of ε but also an impoverishing of E and σ_{max}, a result that can be partially explained by taking into account the possible lowering effect that the relatively more flexible poly(butylene succinate-*co*-glutarate) has on T_g. What it is concluded is that the ionomer is able to produce a positive effect on mechanical properties of the nanocomposites of PBS with cloisite. This result although preliminary is of great relevance since it brings out the suitability of using PBS copolyester ionomers to optimize the preparation of PBS nanocomposites, an approach that offers a wide assortment of technical possibilities.

CONCLUSIONS

$PBS_xG_yG^I_z$ terpolyesters, all they containing 35% of total glutarate and trimethylammonium glutarate units but varying in the ratio in which these two units are present, were synthesized by polymerization in solution using a scandium catalyst. All these terpolyesters were fairly stable to heat and were semicrystalline. Their T_g was close to that of PBS but they showed much poorer mechanical properties, a behavior that is the logical consequence of their low molecular weights. The use of these terpolyesters as compatibilizers in the preparation of nanocomposites made of PBS and cloisite gave outstanding results. Their presence in the nanocomposites in minor amounts gave rise to a significant increase in the Young modulus and the stress to yield and in particular to a large increment in the elongation to break. The capacity of such terpolyester ionomers to enhance the mechanical properties of PBS·CL nanocomposites must be attributed to their unique binding effect based on a combination of their good compatibility with PBS and their strong ionic interaction with the cationically charged layer surfaces of cloisite.

Acknowledgements

The authors would like to acknowledge the financial support received from MINECO MAT2012-38044-CO3-03 project. Authors are also indebted to Universitat Politècnica de Catalunya for the UPC-Research grant awarded to M. Bautista Betancur.

REFERENCES

1. M.S. Nikolic, D. Poleti, and J. Djonlagic, *Eur. Polym. J*., **39**, 2183 (2003).

2. T. Fujimaki, *Polym. Degrad. Stab*., ***59***, 209 (1998).

3. J. Xu, and B.H. Guo, "Microbial Succinic Acid, Its Polymer Poly(butylene succinate),and Applications," in: Plastic from Bacterias: Natural Functions and Applications,. Berlin, Springer-Verlag, 347 (2010).

4. E. Yancheva, D. Paneva, N. Manolova, R. Mincheva, D. Danchev, P. Dubois, and I. Rashkov, *Biomacromolecules*, **11**, 521 (**2010)**.

5. Y. He, X.T. Shuai, K. Kasuya, Y. Doi, and Y. Inoue, *Biomacromolecules*, **2**, 1045 (2001).

6. S.I. Han, J.S. Lim, D.K. Kim, M.N. Kim, and S.S. Im, *Polym. Degrad. Stabil*., **93**, 889 (2008).

7. S.S. Ray, K. Okamoto, and M. Okamoto, *Macromolecules*, **36**, 2355 (2003).

8. Y. Someya, T. Nakazato, N. Teramoto, and M. Shibata. *J. Appl. Polym. Sci*., ***91***, 463 (2004).

9. S.S. Ray, K. Okamoto, P. Maiti, and M. Okamoto, *J. Nanosci. Nanotech*., **2**, 1 (2002).

10. S.S. Ray, and M. Bousmina, M. Okamoto, *Macromol. Mater.. Eng.,* **290**, 759 (2005).

11. M. Hara, and J.A. Sauer, *Macromol. Chem. Phys*., **34**, 325 (1994).

12. G.D. Barber, B.H. Calhoun, and R.B. Moore, *Polymer*, **46**, 6706 (2005).

13. S.I. Han, Y.T. Yoo, D.K. Kim, and S.S. Im, *Macromol. Biosci*., **4**, 199 (2004).

14. S.I. Han, S.S. Im, and D.K. Kim, *Polymer*, **44**, 7165 (2003).

15. C.M. Chen, and N. Leo Benoiton, *Can. J. Chem*., **54**, 3310 (1976).

16. A. Takasu, Y. Iio, Y. Oishi, Y. Narukawa, and T. Hirabayashi, *Macromolecules*, **38**, 1048 (2005).

17. N.N. Bhiwankar, and R.A. Weiss, *Polymer*, **47**, 6684 (2006).

18. C. Lavilla, A. Alla, A. Martínez de Illarduya, S. Muñoz-Guerra, *Biomacromolecules*, **14**, 781 (2013).

19. S.K. Lim, J.J. Lee, S.G. Jang, S.I. Lee, and K.H. Lee, *Polym. Eng. Sci*., **54**, 1316 (2011).

20. K. Okamoto, S.S. Ray, and M. Okamoto, *J. Polym. Sci. Part B: Polym. Phys*., **41**, 3160 (2003).

21. S.S. Ray, and M. Bousmina, *Polymer*, **46**, 12430 (2005).

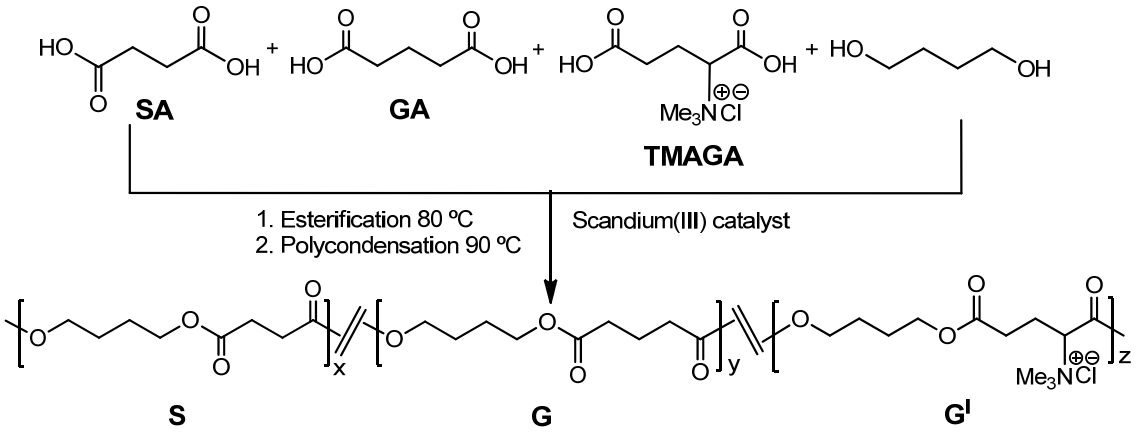

Scheme I. Polymerization reactions leading to $PBS_xG_yG^{I}_z$ terpolyesters.

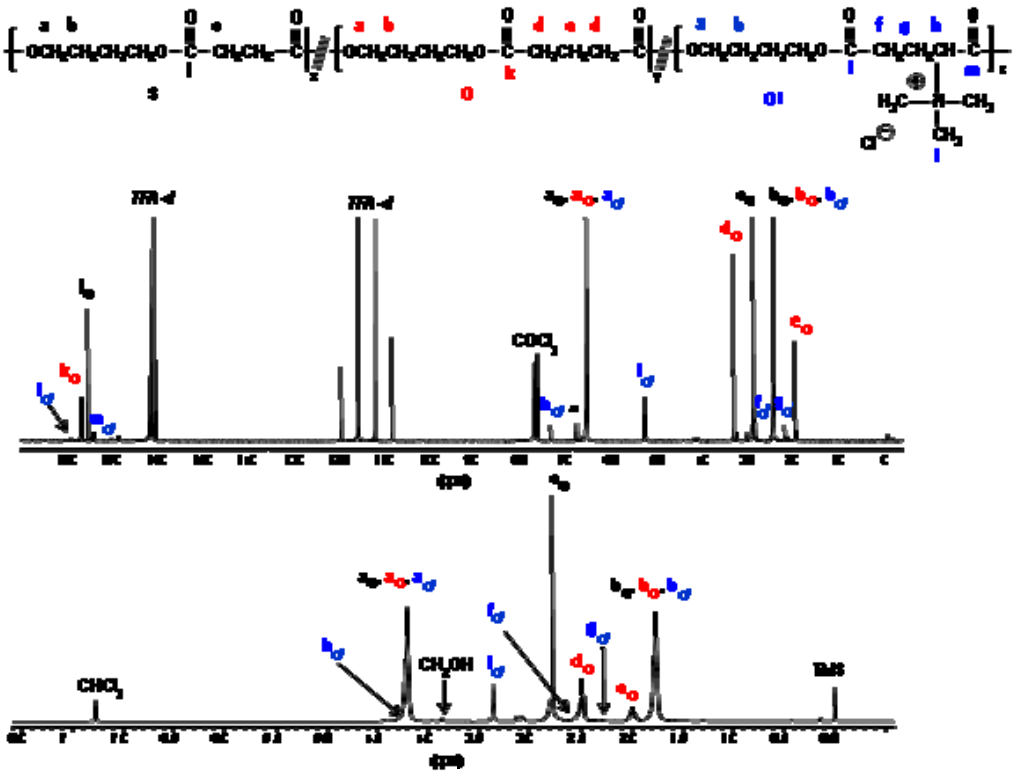

Figure 1. ^{13}C NMR (top) and ^{1}H NMR (bottom) of $PBS_{65}GT_{25}G^{I}_{10}$ terpolyester. (*) CH_2OH end groups.

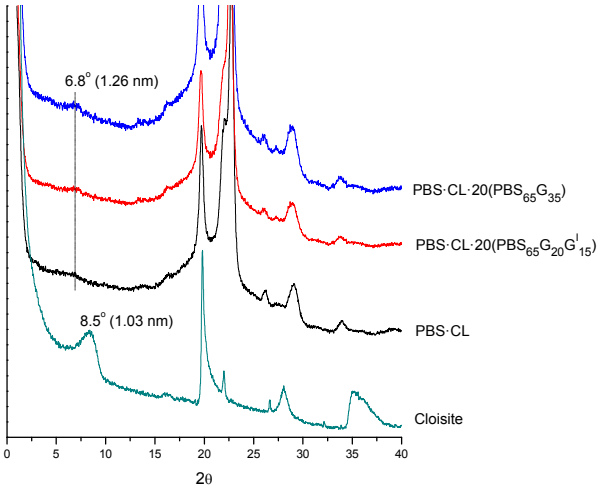

Figure 2. Powder XRD profiles recorded from nanocomposites and cloisite.

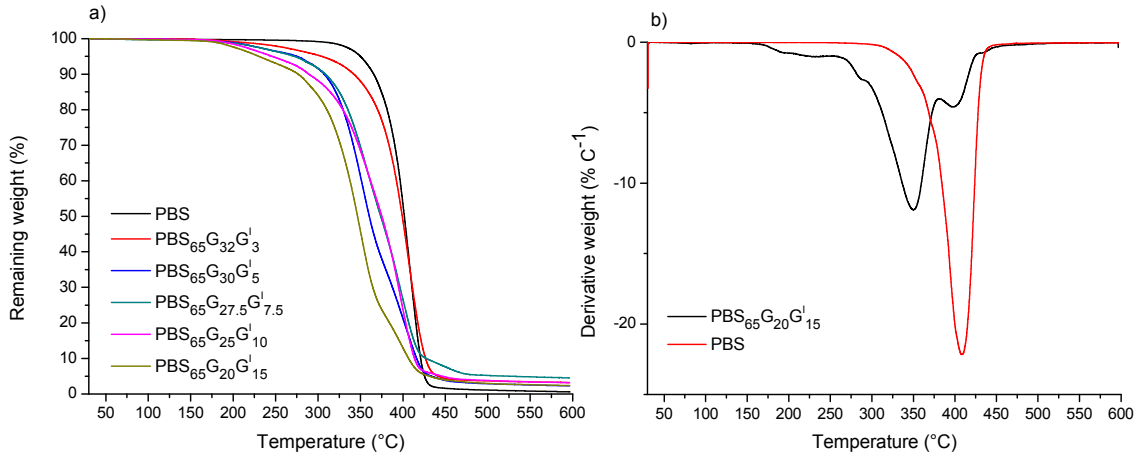

Figure 3. TGA traces of PBS and $PBS_xG_yG'_z$ terpolyesters (a). Derivative curves of PBS and $PBS_{65}G_{20}G'_{15}$.

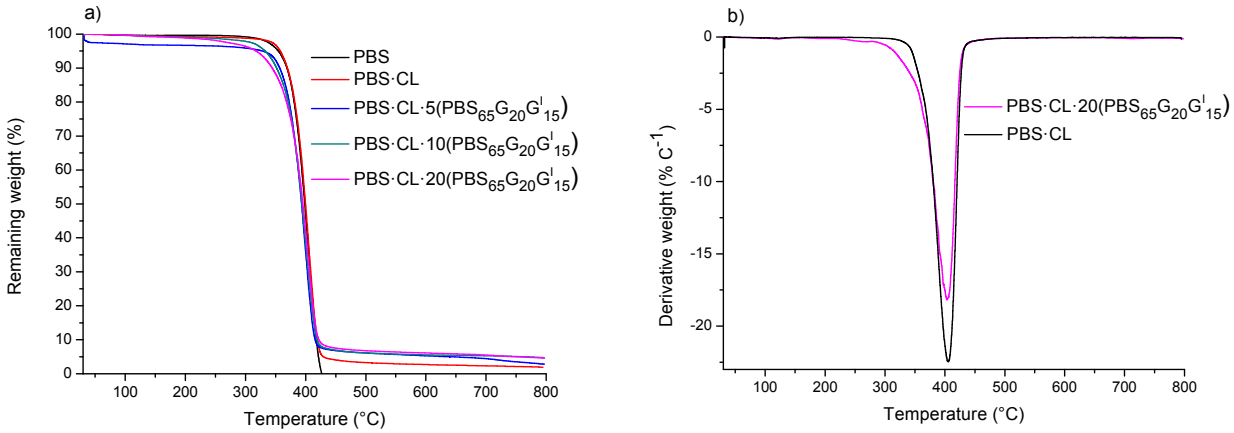

Figure 4. TGA traces of PBS and PBS·CL·w%$PBS_xG_yG'_z$ nanocomposites (a). Derivative curves of PBS and PBS·CL·20%$PBS_{65}G_{20}G'_{15}$ nanocomposite.

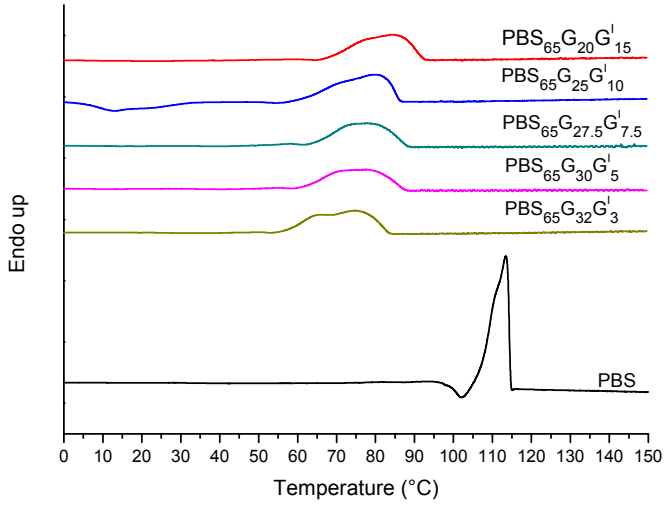

Figure 5. DSC thermograms (second heating) PBSx$G_yG'_z$ terpolyesters.

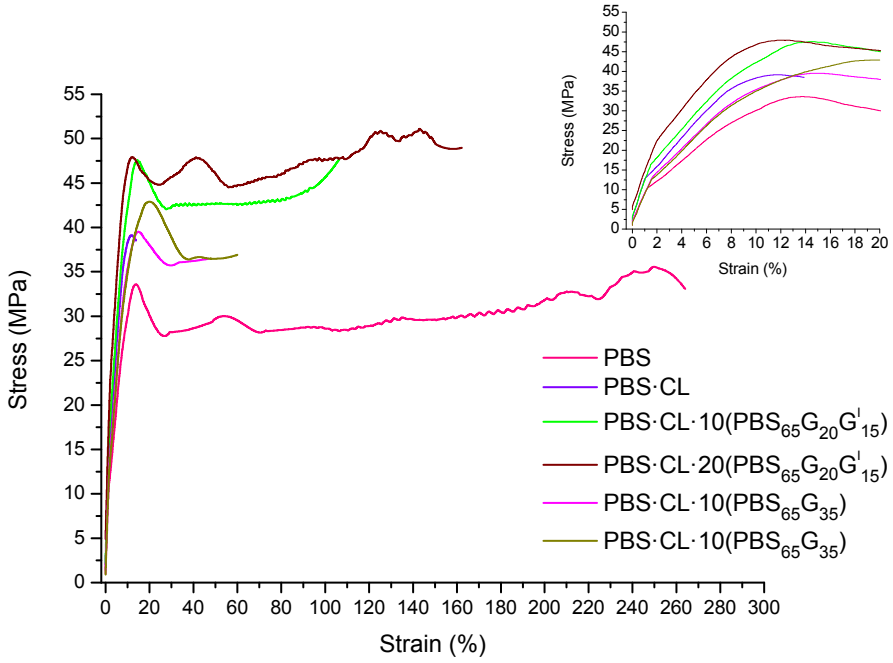

Figure 6. Stress-strain traces of nanocomposites. The curve obtained from PBS is also included for comparison.

Table 1. Composition and molecular weights of PBS and $PBS_xG_yG^I_z$ terpolyesters.

Copolyester	Composition		Molecular weight		
	S/G/G^I[a]	S/G/G^I[b]	$[\eta]$[c]	M_w[d]	$Đ$[d]
PBS	100/0/0	100/0/0	1.33	112,000	2.2
$PBS_{65}G_{32}G^I_3$	65/32/3	66.4/31/2.6	0.43	10,300	2.1
$PBS_{65}G_{30}G^I_5$	65/30/5	64.3/29.7/5.9	0.44	10,600	2.2
$PBS_{65}G_{27.5}G^I_{7.5}$	65/27.5/7.5	65.6/27.8/6.6	0.42	10,400	2.3
$PBS_{65}G_{25}G^I_{10}$	65/25/10	67/24.8/8.2	0.41	10,200	2.5
$PBS_{65}G_{20}G^I_{15}$	65/20/15	67.8/19.9/12.3	0.41	9,500	2.5

[a] Molar ratio of monomers in the feed.
[b] Molar composition of the terpolyester determined by ^{1}H NMR.
[c] Intrinsic viscosity (dL·g^{-1}) measured in dichloroacetic acid at 25 ºC.
[d] Weight-average molecular weight (M_w) (g·mol^{-1}) and dispersity ($Đ$) determined by GPC.

Table 2. Thermal and mechanical properties of PBS homopolymer and $PBS_xG_y G^I_z$ terpolyesters.

	TGA			DSC					Stress-strain parameters		
	$^{o}T_d$[a]	$^{max}T_d$[b]	RW[c]	T_g[d]	T_m[e]	ΔH_m[e]	T_c[f]	ΔH_c[f]	E[g]	σ_{max}[h]	ε_{max}[i]
Terpolyester	(ºC)	(ºC)	(%)	(ºC)	(ºC)	(Jg^{-1})	(ºC)	(Jg^{-1})	(Mpa)	(Mpa)	(%)
PBS	363	408	1	-37	115 (114)	70 (74)	75	66	440±5	35±1	282±10
$PBS_{65}G_{32}G^I_3$	342	408	2.1	-45	71 (75)	51 (39)	26	39	149±2	2.23±0.3	0.30±0.1
$PBS_{65}G_{30}G^I_5$	310	**352**/400	2.3	-41	74 (78)	51 (34)	30	37	152±3	2.66±0.5	0.42±0.3
$PBS_{65}G_{27.5}G^I_{7.5}$	309	357/**395**	3.2	-40	76 (78)	52 (34)	31	36	165±5	3.12±0.3	0.76±0.2
$PBS_{65}G_{25}G^I_{10}$	291	356/**395**	3.4	-38	82 (82)	54 (44)	25	44	174±6	3.34±0.2	0.87±0.4
$PBS_{65}G_{20}G^I_{15}$	276	**350**/398	2.8	-38	82 (83)	55 (38)	35	38	266±3	5.05±0.3	1.46±0.4
Nanocomposite											
PBS·CL	370	**406**	2	-38	114 (113)	61 (48)	90	60	607±7	41±4	16±0.5
PBS·CL·5($PBS_{65}G_{20}G^I_{15}$)	356	**400**	2.7	-38	114 (113)	61 (60)	88	58	713±15	50±2	25±3
PBS·CL·10($PBS_{65}G_{20}G^I_{15}$)	353	**401**	4.8	-40	114 (113)	60 (57)	85	59	747±15	49±3	109±20
PBS·CL·20($PBS_{65}G_{20}G^I_{15}$)	345	**404**	4.9	-40	115 (113)	60 (57)	85	59	731±10	48±5	144±15
PBS·CL·10($PBS_{65}G_{35}$)	350	**403**	2.7	-39	114 (113)	55(54)	80	56	550±10	39±1	40±5
PBS·CL·20($PBS_{65}G_{35}$)	349	**401**	2.9	-39	114(113)	53(52)	78	52	560±15	44±1	60±5

[a]Degradation temperature at which a 10% weight loss was observed in TGA traces at 10 ºC·min^{-1}.
[b]Temperature of maximum degradation rate (in bold main degradation temperature).
[c]Remaining weight at 600 ºC for the terpolyester. Remaining weight at 800 ºC for the nanocomposites.
[d]Glass transition temperature taken as the inflection point of the heating DSC traces of melt-quenched samples recorded at 20 ºC·min^{-1}.
[e]Melting temperatures and enthalpies were registered at a heating rate of 10 ºC·min^{-1}. In parenthesis, values recorded in the second heating.
[f]Crystallization temperatures and enthalpies were registered at cooling from 200 ºC at 10 ºC·min^{-1}.
[g]Young's modulus measured at room temperature on a Zwick BZ2.5/TN1S.
[h]Maximum tensile stress.
[i]Maximum elongation at break.